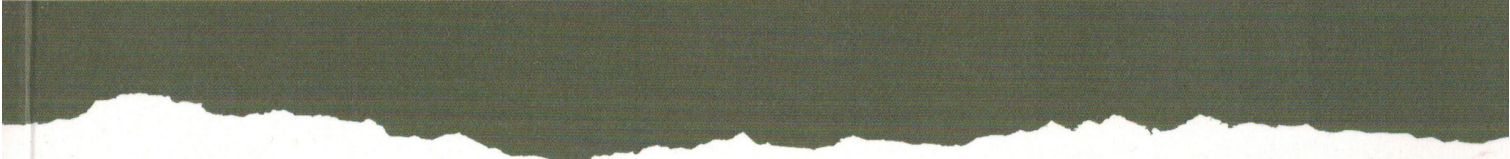


**10th International Symposium
on Mechanics of Materials and Structures**



GUM METAL – A UNIQUE TI ALLOY – INVESTIGATED BY DIGITAL IMAGE CORRELATION AND INFRARED THERMOGRAPHY

Elżbieta A. PIECZYSKA*, Karol GOLASIŃSKI†, Michał MAJ‡, Maria STASZCZAK*, Shigeru KURAMOTO**, Tadahiko FURUTA***

*Department of Experimental Mechanics, Institute of Fundamental Technological Research, PAS, Pawińskiego 5 B, 02-106 Warsaw, Poland

†Department of Mechanical Engineering, Ibaraki University; 4-12-1, Nakanarusawa, Hitachi, 316-8511, Japan

‡Toyota Central Research & Development Laboratories, Inc., Nagakute, Aichi, 480-1192, Japan

epiecz@ippt.pan.pl, kgolasin@ippt.pan.pl, mimai@ippt.pan.pl, mstasz@ippt.pan.pl, shigeru.kuramoto.11@vc.ibaraki.ac.jp,
e0646@mosk.tytlabs.co.jp

Key words: Advanced material, Titanium alloy, Gum Metal, Superelasticity, High strength, Tension, Infrared camera, DIC

1. INTRODUCTION

Gum Metal is a β -Ti alloy with outstanding mechanical properties such as relatively low Young's modulus (c. 65 GPa), large reversible deformation (c. 2%) and high strength (c. 1000MPa). These properties are related to the specific chemical composition of the alloy, usually Ti–23Nb–0.7Ta–2Zr–1.2O (at.%), and is usually cold-worked up to 90% in area reduction. The research concerns investigation of thermodynamic nature of the recoverable deformation of Gum Metal [Saito et al., 2003, Kuramoto et al., 2006]. To this end, a combination of Digital Image Correlation (DIC) and Infrared Thermography (IRT) were used during the tensile loading of Gum Metal [Pieczyska et al., 2016, 2018; Golasiński et al., 2017].

2. EXPERIMENTAL DETAILS

The setup used in this investigation is shown in Fig. 1. It consisted of an MTS 858 TM and two cameras working in two different spectral ranges: visible (0.3-1 μm) Manta G-125B and IR (3-5 μm) ThermoCam Phoenix. Dog bone sample with sizes 100 x 8 x 0.5 mm were used, gauge part 7 x 4 mm; length of virtual extensometer for DIC - 7 mm. More experimental data for investigation of effects of thermomechanical couplings in Gum Metal under tensile loading is presented in [Pieczyska et al., 2018].

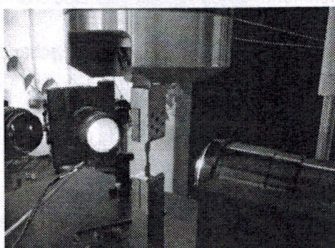


Fig. 1. Experimental setup used for investigation of mechanical and thermal characteristics of Gum Metal

Gum Metal specimen was subjected to tension on a testing machine up to rupture at two strain rates 10^{-1}s^{-1} and 10^{-2}s^{-1} . Displacement and strain distributions were determined on the basis of DIC algorithm.

3. RESULTS AND DISCUSSION

The stress σ and mean temperature changes (ΔT_{mean}) of the Gum Metal specimen vs. strain, obtained during tension at strain rate 10^{-2}s^{-1} up to strain 0.025, is shown in Fig. 2. It was confirmed that the alloy is characterized by relatively low Young's modulus (c. 65 GPa), large reversible deformation (c. 1.6%) and high strength (c. 1000 MPa).

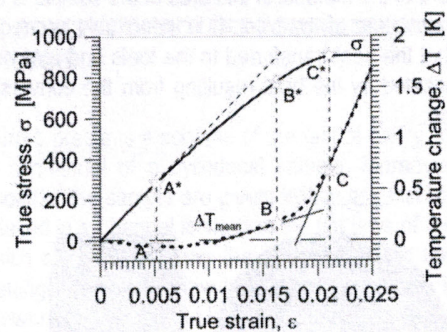


Fig. 2. Stress σ and temperature change (ΔT_{mean}) vs. strain ϵ obtained for Gum Metal's tension up to 0.025 at strain rate 10^{-2}s^{-1}

Moreover it was found that the elastic yield limit, corresponding to maximal drop in the specimen temperature (A'), and limit of mechanically reversible deformation (B'). Increase in the specimen temperature (after it drops due to thermoelastic effect) started from point A. It revealed dissipative character of the process, probably caused by stress-induced phase of α'' phase nanodomains [Pieczyska et al., 2018].

The stress σ and mean temperature changes ΔT_{mean} versus strain ε for the initial stage of tension at higher strain rate of $10^{-1} s^{-1}$ is shown in Fig. 3. In the same figure, strain distributions in the direction of tension ε_y obtained by the DIC algorithm and temperature distributions obtained by IRT are presented.

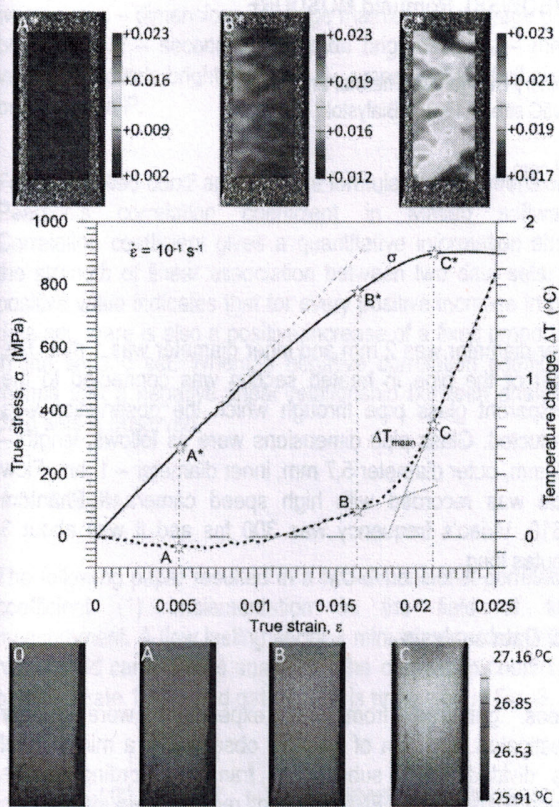


Fig. 3. Stress σ and temperature change ΔT_{mean} vs. strain ε for Gum Metal's tension in the initial deformation range at strain rate of $10^{-1} s^{-1}$ with strain distributions (above; A*-C*) and thermograms (below; 0, A-C)

The thermogram marked by 0 denotes the temperature distribution before the specimen loading. The marked points A*-A, B*-B, and C*-C denote the stress and temperature values corresponding to the Gum Metal's elastic limit, the limit of the mechanically reversible deformation, and the start of almost linear, significantly higher increase in temperature, respectively.

It can be noticed, that the thermal response in the initial loading range reaches its minimal value (points A-A*) significantly before the end of the nonlinear reversible deformation of Gum Metal (points B-B*) as shown in Fig. 3.

Based on the obtained mechanical and thermal characteristics, the subsequent stages for the Gum Metal loading can be distinguished (Tables 1, 2):

0 - A* - elastic deformation stage, accompanied by drop in temperature,

A* - B*- superelastic-like deformation, characterized by dissipative mechanisms

B* - C* - yielding, accompanied by fast growth of temperature.

Tab. 1. Gum Metal loading stages based on stress-strain curve

Points	Stage
0 - A*	Elastic deformation
A* - B*	Superelastic-like deformation
B* - C*	Yielding

Tab. 2. Gum Metal loading stages based on temperature change

Points	Stage
0 - A	Thermoelastic effect
A - B	Dissipative mechanisms
B - C	Fast growth

4. CONCLUSIONS

The mechanical characteristics confirmed the Gum Metal's large nonlinear superelastic-like behavior, low elastic modulus, and high strength, while the related temperature changes provided new thermodynamic data for analysis of the alloy's elastic-plastic transition and development of the strain localization leading to the necking and rupture.

It was found that irrespective of the applied strain rate the maximal drop in the Gum Metal's temperature (thermoelastic effect) occurs significantly earlier than the limit of its mechanically reversible deformation.

The increase in the specimen temperature between the maximal drop and mechanically reversible stage reveals a dissipative character of the deformation in this range.

REFERENCES

1. Golasiński K.M., Pieczyska E.A., Staszczak M., Maj M., Furuta T., Kuramoto S. (2017), Infrared thermography applied for experimental investigation of thermomechanical couplings in Gum Metal, *Quantitative InfraRed Thermography Journal*, Vol.14, 226-233.
2. Kuramoto S., Furuta T., Hwang J., Nishino K, Saito T. (2006), Elastic properties of Gum Metal, *Materials Science and Engineering: A*, Vol. 442, 454-457.
3. Pieczyska E.A., Maj M., Golasiński K., Staszczak M., Furuta T., Kuramoto S. (2018), Thermomechanical Studies of Yielding and Strain Localization Phenomena of Gum Metal under Tension, *Materials*, Vol. 11, 567.
4. Pieczyska, E.A.; Maj, M.; Furuta, T.; Kuramoto, S. (2016), Gum Metal- unique properties and results of initial investigation of a new titanium alloy - extended paper. In *Advances in Mechanics: Theoretical, Computational and Interdisciplinary*; Kleiber, M., Burczyński, T., Wilde, K., Górski, J., Winkelmann, K., Smakosz, Ł., Eds.; CRC Press/Balkema, 469-472, Taylor & Francis: London.
5. Saito, T.; Furuta, T.; Hwang, J.H., Kuramoto, S.; Nishino, K.; Suzuki, N.; Chen, R.; Yamada, A.; Ito, K.; Seno, Y.; Nonaka, T.; Ikehata, H.; Nagasako, N.; Iwamoto, C.; Ikuhara, Y.; Sakuma, T. (2003), Multifunctional Alloys obtained via a dislocation free plastic deformation mechanism, *Science*, 2003, Vol. 300, 464-467.

Acknowledgements

The research was supported by the National Science Centre, Poland; under Projects: 2014/13/B/ST8/04280, 2016/23/N/ST8/03688 and 2017/27/B/ST8/03074.